

MODELING A VIBRATING STRING TERMINATED AGAINST A BRIDGE WITH ARBITRARY GEOMETRY

Dmitri Kartofelev, Anatoli Stulov
Institute of Cybernetics at
Tallinn University of Technology,
Tallinn, Estonia
dima@cs.ioc.ee

Heidi-Maria Lehtonen, Vesa Välimäki
Department of Signal Processing and
Acoustics, Aalto University,
Espoo, Finland
heidi-maria.lehtonen@aalto.fi

ABSTRACT

This paper considers dynamic string motion in which the displacement is unilaterally constrained by the termination condition with an arbitrarily chosen geometry. A digital waveguide model is proposed for simulating the nonlinearity inducing interactions between the vibrating string and the contact condition at the point of string termination. The current work analyzes the resulting string motion influenced by the contact conditions with mostly flat but slightly curved geometries. The effect of a minute imperfection of the termination condition on the string vibration is investigated. It is shown that the lossless string vibrates in two distinct vibration regimes. In the beginning the string starts to interact in a nonlinear fashion with the bridge, and the resulting string motion is nonperiodic. The duration of that vibration regime depends on the geometry of the bridge. After some time of nonperiodic vibration, the string vibration settles in a periodic regime. Presented results are applicable for example in the physics-based sound synthesis of stringed musical instruments, such as the shamisen, biwa, sitar, tambura, veena or even the bray harp and the grand piano.

1. INTRODUCTION

In numerous musical instruments the collision of a vibrating string with rigid spatial obstacles, such as frets or a curved bridge, are crucial to the tonal quality of the produced sounds. Lutes such as the shamisen, biwa, sitar, tambura or veena have a very distinctive sound which can be described as *buzzing*. The form of the bridge used in these instruments is quite different from that usually found in most stringed instruments, since the profiles of the bridges are slightly curved, almost flat (see Fig. 1). The spatial extent of the bridges along the direction of the string is relatively large compared to the speaking length of the strings themselves [1].

A similar mechanism is also not unknown in Western instruments. The treble strings of a grand piano usually terminate at the capo bar (*capo d'astro*). The V-shaped sec-

tion of the capo bar has a parabolic curvature, and although the area to which the string rapidly touches while vibrating is small compared to the string's speaking length, it was shown by Stulov and Kartofelev [2] that the capo bar has a noticeable effect on the piano tone formation.

Also the Medieval and Renaissance bray harp has small bray-pins which provide a metal surface for the vibrating string to impact, increasing the upper partial content in the tone and providing a means for the harp to be audible in larger spaces and in ensemble with other instruments [3]. It is evident that for realistic physically informed modeling of these instruments such nonlinearity inducing interactions need to be examined and simulated accurately.

Raman was the first to study the effect and identify the bridge as the main reason for distinctive sounding of the tambura and veena [4]. Over the years many authors have solved this problem using different approaches [3], [5] – [15]. An overview and comparison of the existing methods that are proposed for modeling the interaction between the termination and the string are presented by Vyasarayani, *et al.* in [3].

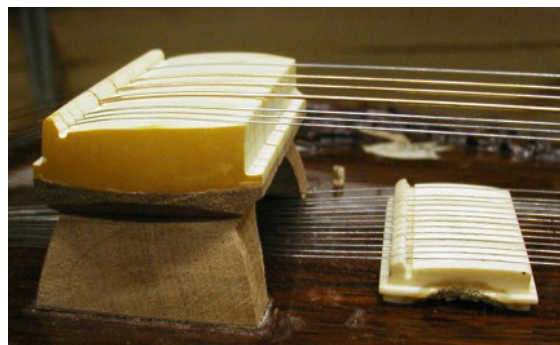


Figure 1. *Jawari*, the main bridge of the sitar and *taraf ka ghoraj*, the sympathetic string bridge.

The aim of the current paper is to model the vibration of the string which is unilaterally constrained at one of the points of string termination. Dynamic motion of the plucked ideal string against the termination condition (TC) with three different profile geometries are simulated and obtained results are examined. In addition, a method for quantifying the effect of minute geometric imperfections of the mostly flat bridge on the string vibration is provided.

Although the cases examined here are for bridges with mostly flat profile geometries, the obtained conclusions hold

to some degree for cases where the bridge profile geometries are more versatile, cf. [2].

Compared to the previously published work, we propose a new and relatively simple approach for modeling the non-linear bridge-string interaction and consequently the dynamic motion of the entire string. In this work the proposed model is demonstrated using physical parameters that are obtained from a Chinese lute biwa, thus presenting an applied approach.

2. IDEAL STRING

For analyzing the phenomenon of interest, it is sufficient to describe the dynamic motion of the string using the *ideal* string. Phenomena such as losses or dispersion are discarded. We consider the wave equation for the linear and lossless flexible string:

$$\frac{\partial^2 u}{\partial t^2} = c^2 \frac{\partial^2 u}{\partial x^2} \quad (1)$$

with $u(0, t) = u(L, t) = 0$, where L and $u(x, t)$ are the speaking length and the displacement of the string, respectively. In (1) the value $c = \sqrt{T/\mu}$ is the speed of the traveling waves on the string, where T is the tension and μ is the linear mass density of the string [16].

String parameters for all the calculations in the current paper are the same as used by Taguti in [8]. Taguti investigated a biwa string with the following parameters: string length $L = 0.8$ m; linear mass density $\mu = 0.375$ g/m; string tension $T = 38.4$ N. From here it follows that the speed of the traveling waves along the string is $c = 320$ m/s and the fundamental frequency of such a string is $f_0 = 200$ Hz.

3. STRING EXCITATION

The string plucking condition can be introduced as follows. We assume that at the point $x = l = 3/4L$ the emerging traveling wave is of the form

$$u(l, t) = \begin{cases} A \left(\frac{t}{t_0}\right)^2 e^{2(1-t/t_0)}, & \text{if } 0 \leq t \leq t_0, \\ A, & \text{if } t > t_0. \end{cases} \quad (2)$$

In (2) $A = 1$ cm is the amplitude of the outgoing traveling wave and the duration of the excitation is $t = t_0 = 4$ ms. Selection of the plucking condition (2) ensures that the plucking force acting on the string point $x = l$ ceases if $t \geq t_0$ (time derivative of (2) is proportional to the plucking force) [2].

It can be shown that (1) may be satisfied by superposition of nondispersive traveling waves $u_r(t - x/c)$ and $u_l(t + x/c)$ moving in either directions along the string emerging from the plucking point $x = l$. At this point $u_r(l, t) = u_l(l, t) = u(l, t)$. These two waves u_r and u_l are simply a translation of the plucking condition (2) from the point $x = l$ to other segments of the string [16].

In the case of ideal rigid string termination where no TC is present, the boundary value $u(0, t) = u(L, t) = 0$ is satisfied if the wave $u_r(t - x/c)$ propagating to the right at the

point $x = L$ creates the wave $u_l(t + x/c) = -u_r(t - x/c)$ moving to the left and the wave $u_l(t + x/c)$ propagating to the left at the point $x = 0$ creates the wave $u_r(t - x/c) = -u_l(t + x/c)$ moving to the right. This procedure can be interpreted as equivalent to the digital waveguide approach [17, 18, 19].

It follows that for the current model the string displacement $u(x, t)$ at any point x of the string and for all time instants t is simply the resulting sum of waveforms u_r and u_l moving in both directions

$$u(x, t) = u_r\left(t - \frac{x}{c}\right) + u_l\left(t + \frac{x}{c}\right). \quad (3)$$

The method for modeling the bridge-string interaction is explained in Sections 5 and 6.

4. BRIDGE GEOMETRY

Slightly curved bridges of the lutes mentioned in Section 1 are usually located at the far end of the neck. Similarly the geometric contact condition (TC) is located at the termination point of the string. Figure 2 shows the traveling waves u_r and u_l , string displacement $u(x, t)$, and the location of the rigid termination (bridge) relative to the string.

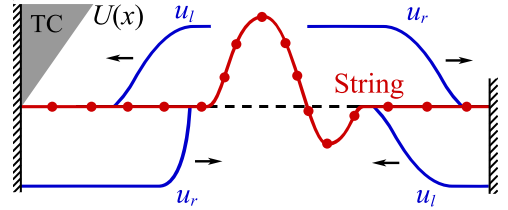


Figure 2. Scheme of the string displacement model. The traveling waves u_r and u_l (solid lines), and the forms of the string (solid lines marked by circles). Position of the TC relative to the string is shown using gray formation.

4.1 Case 1: Linear bridge with a sharp edge

The function $U(x)$ that describes the profile of a flat bridge is calculated as follows

$$U(x) = \begin{cases} kx, & \text{if } x \leq x_c, \\ \infty, & \text{if } x > x_c, \end{cases} \quad (4)$$

where $k = \tan \theta = 0.008$ is the slope of the linear function where $\theta \approx 0.008$ rad $\approx 0.46^\circ$. Value $x_c = 15$ mm marks the coordinate of the truncation of the linear function.

4.2 Case 2: Linear bridge with a curved edge

The profile of a bridge with a curved edge is calculated as follows

$$U(x) = \begin{cases} kx, & \text{if } x \leq x_b, \\ \frac{1}{2R}(x - x_b)^2, & \text{if } x > x_b, \end{cases} \quad (5)$$

where the parameter k has the same value and meaning as in the previous case. Parameter $R = 10$ mm is the curvature radius of the corresponding parabolic function

$f(x) = (2R)^{-1}x^2$ at its minimum. Coordinate $x_b = 10$ mm marks the transition between linear and parabolic parts of the geometry.

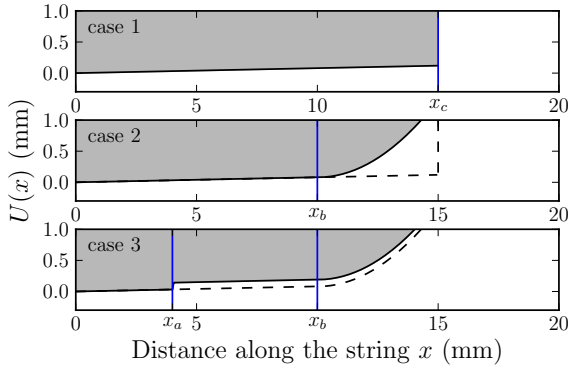


Figure 3. Termination condition geometry for the cases under study. Solid vertical lines mark the positions of the characteristic values x_a , x_b and x_c . Case 1: linear bridge with a sharp edge. Case 2: linear bridge with a curved edge, the dashed line shows the profile of the case 1 for comparison. Case 3: bridge with a small geometric imperfection, the dashed line shows the case 2 for comparison.

4.3 Case 3: Bridge with a geometric imperfection

The bridge in this case is similar to the previous case with the exception of an addition of small imperfection in the form of discontinuity in the linear part of the TC in (5). The bridge profile geometry for this case can be expressed in the following form

$$U(x) = \begin{cases} kx, & \text{if } x \leq x_a, \\ kx + y, & \text{if } x_a < x \leq x_b, \\ \frac{1}{2R}(x - x_b)^2 + K, & \text{if } x > x_b, \end{cases} \quad (6)$$

where the parameters k and R have the same value and meaning as in the previous cases. Parameter $y = 0.11$ mm raises the value of linear function in the interval $x = (x_a, x_b]$ where $x_a = 4$ mm and $x_b = 10$ mm. Constant $K = kx_b + y$ is presented in order to preserve continuity of the form in vicinity of the point $x = x_b$.

The TC geometries presented in (4) - (6) are shown in Fig. 3.

5. BRIDGE-STRING INTERACTION MODEL

In order to model the bridge-string interaction we assume that the reflecting wave $u_r(t - x/c)$ moving to the right appears only at the point $x = x^*$, where the amplitude of the string deflection $u(x^*, t) \geq U(x^*)$. The position of this point x^* is determined by the TC geometry $U(x)$ in the following way. Since the termination is rigid we must have $u(x^*, t) = U(x^*)$, and this condition results in the appearance (addition) of reflected wave

$$u_r\left(t - \frac{x^*}{c}\right) = U(x^*) - u_l\left(t + \frac{x^*}{c}\right), \quad (7)$$

where the waves u_l and u_r correspond to any waves that have reflected on earlier time moments and are currently located at $x = x^*$. The proposed method ensures that the amplitude of the string deflection, which is determined by (3), will never exceed the value $U(x)$.

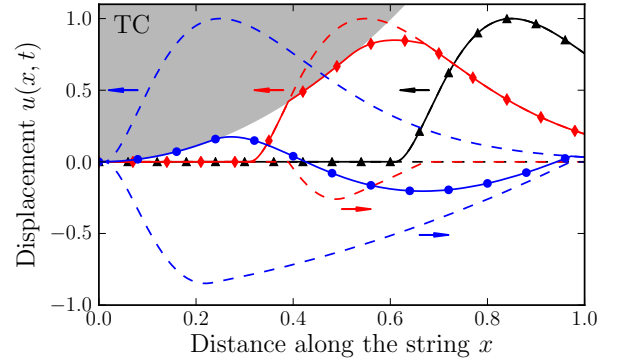


Figure 4. Reflection of the first wave from the termination. The traveling waves u_r and u_l (dashed lines), and the forms of the string (solid lines marked by signs) shown for consequent nondimensional moments of times $t_1 = 0.4$ (triangle); $t_2 = 0.7$ (diamond); $t_3 = 1.0$ (circle).

In Fig. 4 we demonstrate the form of the string in vicinity of the geometric termination during the reflection of the first wave $u_l(t + x/c)$ only. Using the procedure described above, the string deflection as a function of the nondimensional distance along the string is computed for three consequent normalized nondimensional ($c = 1$) moments of time. At the moment $t = t_1$ the form of the string (solid line marked by triangles) is determined only by the traveling wave u_l . At the next moment $t = t_2$ the small segment of the string is in contact with the surface of the termination, and the reflected wave $u_r(x, t_2)$ has appeared (dashed line). The corresponding form of the string deflection is shown by solid line marked with diamonds. At the moment $t = t_3$ the string is in contact with the surface of the termination on the segment closer to the string edge ($x = 0$). The form of the string at this moment is shown by solid line marked with circles, and the reflected wave $u_r(x, t_3)$ is also shown by the dashed line. Thus at some moments the string wraps or clings to the termination, and during that time the form of the string on some segment simply repeats the form of the termination.

6. NUMERICAL IMPLEMENTATION

The bridge-string interaction model and the ideal string vibration are implemented numerically by using discrete t - x space with the time mesh Δt and the space mesh Δx . Values for the Δt and Δx are selected so that

$$c \frac{\Delta t}{\Delta x} = 1, \quad (8)$$

where $c = \sqrt{T/\mu}$. Selection of the step-sizes Δx and Δt according to (8) ensures maximum accuracy of the result for any given resolution of the computational grid. Thus,

the transmission of the traveling waves u_r and u_l with respect to the points of the discrete t - x space are

$$u_r(x_n, t_m) = u_r(x_{n-1}, t_{m-1}), \quad (9)$$

$$u_l(x_n, t_m) = u_l(x_{n+1}, t_{m-1}), \quad (10)$$

where the index $n = 0, \dots, N$ corresponds to the discrete space points and the index $m = 0, \dots, M$ corresponds to the discrete time points. Values of the corresponding coordinates x and t in (9) and (10) can be calculated as $x = x_n = n\Delta x$ and $t = t_m = m\Delta t$, respectively.

In order to satisfy the boundary condition at the right side of the string, namely $u(L, t) = 0$, the mechanism presented in Sec. 3 is used. For every successive time moment t_m

$$u_l(x_N, t_m) = -u_r(x_N, t_{m-1}), \quad (11)$$

where $x_N = N\Delta x = L$.

The effect of the geometric TC on the string vibration can be implemented numerically as follows. According to Sec. 5 the traveling wave u_r only appears in the vicinity of the bridge at the discrete point $x_n = x_n^*$ where the amplitude of the string deflection $u(x_n^*, t) \geq U(x_n^*)$. Thus, for every successive time moment t_m and for all x_n^*

$$u_r(x_n^*, t_m) = u_r(x_n^*, t_m) - \Delta u, \quad (12)$$

where $\Delta u = u(x_n^*, t_m) - U(x_n^*)$. Expression of the form (12) is more suitable for the iterative numerical scheme used to generate the result compared to the expression (7) shown in Sec. 5. Finally, when the aforementioned operations are conducted the final form of the string's displacement with respect to the discrete computational grid takes the form

$$u(x_n, t_m) = u_r(x_n, t_m) + u_l(x_n, t_m). \quad (13)$$

Numerical parameters selected to calculate the presented results are: $\Delta x = 0.985$ mm, $\Delta t = 3.077$ μ s, number of spatial points $N = 816$, including spatial points dedicated for the bridge $N_{TC} = 25$, number of the time points $M = 130000$, from here it follows that the temporal sampling rate is 325 kHz. The relevant part of the computer code written using the Python programming language is available for examination at the supplementary web page of this article [20].

7. RESULTS AND DISCUSSION

Figure 5 shows the time series of the string deflection $u(l, t)$ computed at the plucking point $x = l$. Visual inspection of the string deflection $u(l, t)$ reveals that for all the presented cases the strings vibrate in two distinct regimes. The strong influence of the bridge on the string's motion is noticeable for a certain period of time, and its duration depends on the bridge geometry. During this time prolonging for $t = t_{np}$ the string vibrates in *nonperiodic regime*. One can clearly see that after the moment $t = t_{np}$ the behavior of the deflection $u(l, t)$ becomes seemingly highly periodic. Closer examination reveals that the string's displacement is actually still slightly changing and therefore is not absolutely

periodic (string continues to interact with the bridge) but the change is small and can be neglected. This regime is called here the *periodic vibration regime*. It must be noted that this almost periodic vibration regime is possible only when the bridge profile is mostly flat and the string is considered ideal and lossless.

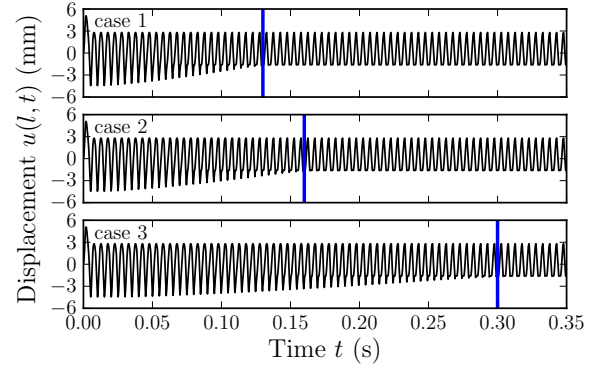


Figure 5. Time series of the string deflection $u(l, t)$ for the cases 1, 2, and 3. Nonperiodic and periodic vibration regimes are separated by vertical lines corresponding to the time moment $t = t_{np}$.

Table 1 shows the corresponding durations of the nonperiodic vibration regimes t_{np} for the cases under study. In addition, the corresponding number of string deflection $u(l, t)$ periods P_{np} are shown.

	t_{np} (s)	P_{np}
Case 1	0.13	26
Case 2	0.16	32
Case 3	0.30	60

Table 1. The duration and the number of the string deflection periods of the nonperiodic vibration regime.

The transitions between the nonperiodic and periodic regimes presented in Fig. 5 are also visible in the spectrograms presented in Fig. 6. All spectrograms are calculated using the Hanning window of the size 45 ms and the overlap value 55% of the window size. The animations of the simulated string vibration terminated against the bridges with profile geometries described in (4) – (6), are available for download on the supplementary web page of the current article [20].

7.1 Case 1: Linear bridge with a sharp edge

Spectrogram of the signal related to the case 1 is shown in Fig. 6 a. Dashed vertical line corresponds to the duration of the nonperiodic vibration regime t_{np} of the string. It can be seen that during the nonperiodic vibration regime the energy of the lower vibration modes is being transferred to the higher modes. This effect of spectral widening can be noticed when comparing Figs. 6 a and 7. Figure 7 shows the spectrogram of the corresponding linear case where no amplitude limiting TC is applied. Transfer of the energy

from lower to higher vibration modes is a sign of nonlinear behavior resulting from the interaction of the vibrating string and the bridge. This phenomenon is similar to the slapped bass effect [6] and the nonlinear limitation of the string amplitude by the damper in the part-pedaling effect in the grand piano [21, 22]. In the periodic vibration regime ($t > t_{np}$) the spectrum remains constant which is an expected result (*cf.* Fig. 5).

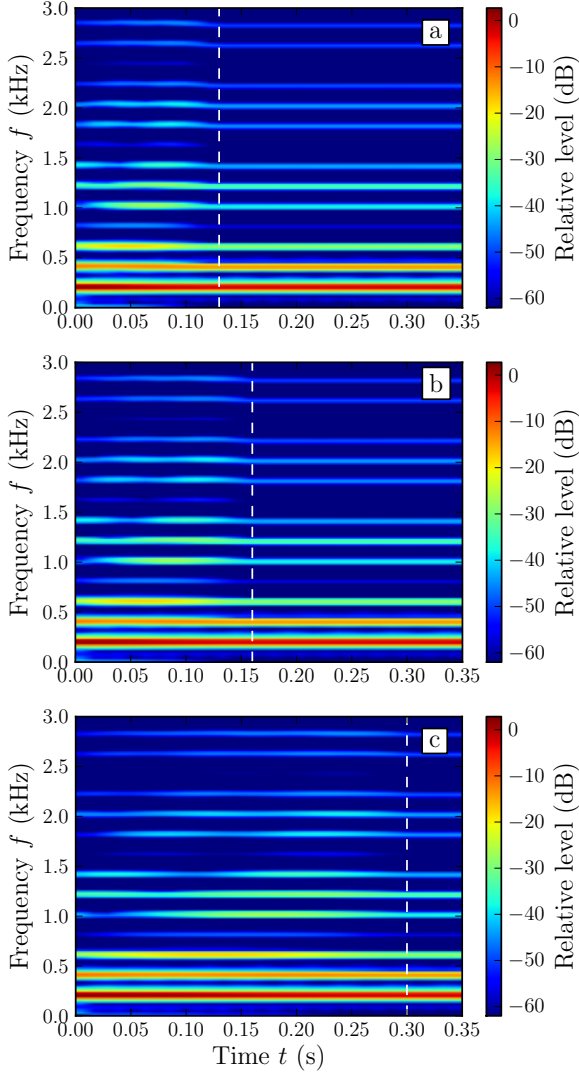


Figure 6. Spectrogram of the signal $u(l, t)$ for the cases: a) case 1, b) case 2 and c) case 3. The transition between nonperiodic and periodic vibration regimes at $t = t_{np}$ is shown using dashed line.

7.2 Case 2: Linear bridge with a curved edge

The spectrogram corresponding to the case 2 is shown in Fig. 6b. As can be seen the result in this case is similar to the case 1 with the exception of the 30 ms longer nonperiodic vibration regime.

7.3 Case 3: Bridge with a geometric imperfection

Figure 6c shows the spectrogram for the case 3. Now the nonperiodic vibration regime is 300 ms long, which is al-

most two times longer compared to the case 2. Again, the energy transfer from lower to higher modes is visible during the nonperiodic vibration regime.

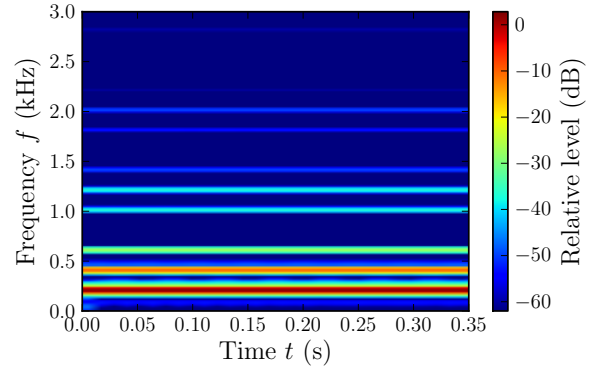


Figure 7. Spectrogram of the signal $u(l, t)$ for the linear case (no TC).

Relatively long nonperiodic vibration regime in connection with the properties of nonlinear dynamic systems can make playing such an instrument challenging. The timbre of the instrument can be very strongly influenced by the selection of the plucking point and the plucking manner, which results in uneven timbre behaviour. This effect is present for example in the sitar, and it makes the learning to play the sitar more complicated compared to the similar Western instruments.

Figure 8 shows four periods of the string deflection $u(l, t)$ during the periodic vibration regime, where the interaction of the string with the bridge is minimal. Figure 8 presents a comparison of all nonlinear cases 1 – 3 to the corresponding linear case. Nonlinear cases are rendered almost identical for $t > t_{np}$. This result is explained by the fact that the selected contact condition profiles defined by (4) - (6) have linear sections near to the string termination point ($x = 0$). With the progression of time this linear section of the bridge *trims* the effects of the other (non-linear) sections of the geometry, thus eventually rendering the periodic string vibrations for all nonlinear cases almost identical.

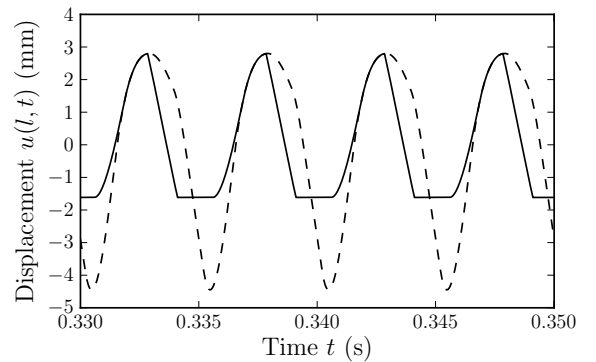


Figure 8. Four periods of the string displacement $u(l, t)$ for the nonlinear cases 1, 2 and 3 are shown using solid line (all identical). Corresponding linear case (no TC) is shown using dashed line.

In addition to the aforementioned results it was noted that a small glide and shift of the fundamental frequency f_0 (and consequently the frequencies of all the other modes, because $f_i = i f_0$ where i is the mode number) of the otherwise harmonic vibration is present. This effect appears for all presented cases and only during the nonperiodic vibration regime after which the frequency slides back to normal (i.e. $f_0 = 200$ Hz). Emergence of this effect is explained by the effective shortening of the speaking length of the string due to the spatial extent of the bridge and the interaction of the string with the bridge.

7.4 String vibration spectrum in the periodic vibration regime

After the period of nonperiodic vibration regime has passed, the string enters the periodic vibration regime. The spectrum of the string vibrations for any time instant of interest is computed using Fourier analysis. If

$$u(x, t) = \sum_i (A_i \cos \omega_i t + B_i \sin \omega_i t) \sin \left(\frac{i\pi x}{L} \right), \quad (14)$$

with normal-mode angular frequencies $\omega_i = i\omega_0$, where $\omega_0 = 2\pi f_0$ and i is the mode number, then

$$A_i = \frac{2}{L} \int_0^L u(x, t) \sin \left(\frac{i\pi x}{L} \right) dx, \quad (15)$$

$$B_i = \frac{2}{L\omega_i} \int_0^L v(x, t) \sin \left(\frac{i\pi x}{L} \right) dx, \quad (16)$$

where $v(x, t)$ is the velocity of the string. It follows that the string mode energy E_i of the i th mode is defined by

$$E_i = \frac{M\omega_i^2}{4} (A_i^2 + B_i^2), \quad (17)$$

where $M = \mu L$ is the total mass of the string. And the mode energy level is defined as

$$EL_i = 10 \log_{10} \left(\frac{E_i}{E_0} \right). \quad (18)$$

Fourier analysis using (18) shows that the spectra of cases 1, 2 and 3 are almost identical for $t > t_{np}$ (cf. Fig. 8). As mentioned earlier this result is explained by the fact that the selected contact condition profiles defined by (4) - (6) have linear sections near to the string termination point ($x = 0$). Figure 9 shows the comparison of the spectrum of the linear case (no TC) with those of the nonlinear cases 1, 2 and 3. The spectrum of the linear case is shown for the time interval $t = (t_0, \infty)$ and the nonlinear cases are shown for the time interval $t = (t_{np}, \infty)$.

Results from spectrogram analysis shown in Fig. 6 are confirmed here by calculations made using (18) and the resulting spectrum is shown in Fig. 9.

Widening of the spectra compared to the linear case and the transfer of energy from lower to higher vibration modes is visible. Relative level of some higher modes grow up to 25 dB. This means that resulting tone of the musical instrument that is equipped with the rigid, slightly curved bridge

which influences the string vibration is completely different from that of an instrument having a regular bridge.

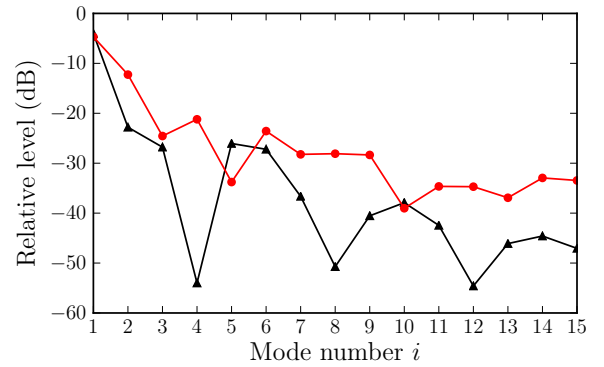


Figure 9. Stationary spectrum of the string vibrations for $t > t_{np}$. Spectra corresponding to the nonlinear cases 1, 2 and 3 are shown using circles (all identical). Linear case (no TC) is shown using triangles.

8. CONCLUSIONS

This article introduced a model that simulates the vibration of an ideal string terminated against a bridge with an arbitrary geometry. Additionally, a method for modeling the effect of minute geometric imperfections of the bridge geometry on the string vibration was presented. It was shown that the lossless string vibrates in two distinct vibration regimes. In the beginning the string starts to interact in a nonlinear fashion with the bridge, and the resulting string motion is nonperiodic. After some time of nonperiodic vibration, the string vibration settles in a *almost* periodic regime, where the dynamic motion of the string is repetitious in time.

The duration of the nonperiodic vibration regime depends on the geometry of the termination. It was concluded that minor imperfection of the bridge profile geometry elongate the duration of the nonperiodic vibration regime and produce noticeable changes in the evolution of the timbre in the nonperiodic regime of vibration. The resulting spectrum in the periodic regime is identical for all nonlinear cases studied. Comparison of the resulting spectra in the periodic vibration regime of the linear and nonlinear cases showed that the interaction of the string with the rigid bridge widens the spectrum by transferring energy from lower to higher vibration modes.

Acknowledgments

This work was conducted in February - April 2013, when Dmitri Kartofelev was visiting Aalto University. His visit was supported by the Kristjan Jaak Scholarship program from the Archimedes Foundation, Estonia.

This research was partly supported by the European Union through the European Regional Development Fund and by the Estonian Ministry of Education and Research (SF 0140 077s08).

The work of Heidi-Maria Lehtonen was supported by the Finnish Cultural Foundation.

The authors are grateful for the useful comments and suggestions from Dr. Balázs Bank.

9. REFERENCES

- [1] Wikipedia the free encyclopedia: “Plucked string instrument,” http://en.wikipedia.org/wiki/Plucked_string_instrument, 2013
- [2] A. Stulov and D. Kartofelev, “Vibration of strings with nonlinear supports,” in press, *Applied Acoustics*, 2013.
- [3] C. P. Vyasrayani, S. Birkett and J. McPhee, “Modeling the dynamics of a vibrating string with a finite distributed unilateral constraint: Application to the sitar,” *J. Acoust. Soc. Am.*, vol. 125, no. 6, pp. 3673–3682, 2009.
- [4] C. V. Raman, “On some Indian stringed instruments,” in *Proc. Indian Assoc. Cultiv. Sci.* vol. 7, pp. 29–33, 1921.
- [5] A. Krishnaswamy and J. O. Smith, “Methods for simulating string collisions with rigid spatial obstacles,” in *Proc. IEEE Workshop on Applications of Signal Processing to Audio and Acoustics*, October 19-22 New Paltz, NY, USA, pp. 233–236, 2003.
- [6] E. Rank and G. Kubin, “A waveguide model for slap-bass synthesis,” in *Proc. IEEE International Conference on Acoustics, Speech, and Signal Processing*, April 21-24, Munich, Germany, pp. 443–446, 1997.
- [7] T. Taguti, “Numerical simulation of vibrating string subject to sawari mechanism,” in *Proc. 19th Int. Congr. on Acoustics*, September 2-7, Madrid, Spain, pp. 1–6, 2007.
- [8] T. Taguti, “Dynamics of simple string subject to unilateral constraint: A model analysis of sawari mechanism,” *Acoustical Science and Technology*, vol. 29, pp. 203–214, 2008.
- [9] R. E. L. Turner and P. Villaggio, “A note on the motion of a string on a unilaterally reacting foundation,” *SIAM Journal on Applied Mathematics*, vol. 49, no. 4, pp. 1223–1230, 1989.
- [10] S. Siddiq, “A physical model of the nonlinear sitar string,” *Archives of Acoustics*, vol. 37, no. 1, pp. 73–79, 2012.
- [11] R. Burrige, J. Kappraff and C. Morshedi, “The sitar string, a vibrating string with a one-sided inelastic constraint,” *SIAM Journal on Applied Mathematics*, vol. 42, no. 6, pp. 1231–1251, 1982.
- [12] S. M. Han and M. A. Grosenbaugh, “Non-linear free vibration of a cable against a straight obstacle,” *Journal of Sound and Vibration*, vol. 273, pp. 337–361, 2004.
- [13] H. Cabannes, “Presentation of software for movies of vibrating strings with obstacles,” *Appl. Math. Lett.*, vol. 10, no. 5, pp. 79–84, 1997.
- [14] C. Valette, “The mechanics of vibrating strings,” in *Mechanics of Musical Instruments*, edited by J. Kergo-
nard and G. Weinreich, Springer-Verlag, Vienna, pp. 115–183, 1995.
- [15] G. Evangelista and F. Eckerholm, “Player–instrument interaction models for digital waveguide synthesis of guitar: touch and collisions,” *IEEE Transactions on audio, speech, and language processing*, vol. 18, no. 4, pp. 822–832, 2010.
- [16] N. H. Fletcher and T. D. Rossing, *The physics of musical instruments*, Springer, 1998.
- [17] J. O. Smith, “Physical Modeling using Digital Waveguides,” *Computer Music Journal*, vol. 16, no. 4, pp. 74–91, 1992.
- [18] V. Välimäki, J. Pakarinen, C. Erkut, and M. Karjalainen, “Discrete-time modelling of musical instruments,” *Reports on Progress in Physics*, vol. 69, no. 1, pp. 1–78, 2006.
- [19] J. O. Smith, *Physical audio signal processing for virtual musical instruments and audio effects*, <https://ccrma.stanford.edu/~jos/pasp/>, W3K Publishing, 2010.
- [20] Supplementary web page of the current article: “Animations of the string vibration terminated against a bridges with arbitrary geometry’s: Cases 1 – 3,” <http://www.cs.ioc.ee/~dima/stringarbitrary.html>
- [21] H.-M. Lehtonen, A. Askenfelt and V. Välimäki, “Analysis of the part-pedaling effect in the piano,” *J. Acoust. Soc. Am.* vol. 126, no. 2, pp. EL49–EL54, 2009.
- [22] A. Stulov, V. Välimäki and H.-M. Lehtonen, “Modeling of the part-pedaling effect in the piano,” in: *Acoustics 2012*, April 23-27, Nantes, France, pp. 1223–1228, 2012.